Elastic period of vibration calculated experimentally in buildings hosting permanent GPS stations

Marco Gatti[†]

Department of Engineering, University of Ferrara, Ferrara 44123, Italy

Abstract: During the earthquake in Emilia (Italy) of 2012, ca. 30 permanent GPS stations were in operation within a radius of about 100 km from the epicenter, each equipped with an antenna rigidly fixed to the host building and sampling the GPS signal at a high rate (> 1 Hz). From the recording of the GPS measurements, the instantaneous displacements s(t) in the North-South and East-West directions of the phase centers of the single GPS antennas at each permanent station during the most important seismic sequences were calculated in kinematic mode. Subsequently, for each of the two displacements considered as two distinct external forces, the elastic response spectra of the building were determined and from them the two periods of vibration T along two orthogonal directions coinciding with the walls of the building were extracted. The experimentally obtained periods of vibration were compared with those inferable from the technical literature. In this way, a sufficiently large sample was obtained per building type, geometry (square, rectangular, regular or irregular planimetry), height (from a minimum of 4 to a maximum of 20 m) and materials (masonry, reinforced concrete, etc.). From the computational point of view, the study confirmed that GPS is an emerging tool for monitoring dynamic displacements and the experimentally estimated value of T is always lower than the one estimated with the formulae reported in the literature. The limitations of the study lie in the impossibility to choose a priori the geometry and/or structural type of the building hosting the GPS station.

Keywords: permanent GPS stations; Emilia-Romagna Italy earthquake; period; vibrations; dynamic structure

1 Introduction

In structural analysis, the elastic period of vibration is one of the global characteristics necessary for evaluation of the external stresses on new or existing buildings resulting from seismic activity. Being related to the seismic demand capacity, it allows the expected performance and thus the safety to be determined.

In general the period of vibration depends on many factors, even though from an analytical point of view it is proportional to the mass and inversely proportional to the stiffness of the structure. The mass closely depends on the planimetric dimensions and the number of floors, while the stiffness is strongly influenced by the structural characteristics of the building and the height.

For this reason, international regulatory codes propose simplified numerical relations for estimation of the period of structures as a function of the height (Chopra, 1995) or the number of floors (NEHRP, 1994), since these two parameters, more than any others, summarize the dependence on the building's mass and stiffness.

These relations have been calculated either numerically, by deriving an interpolating curve from the analysis (elastic or nonlinear) of a set of buildings of the same structural type (ATC, 1978; SEAOC, 1998; CEN, 2004; Chalah *et al.*, 2014), or experimentally by deriving the curve from periods resulting from the analysis of data recorded with accelerometers during monitoring of buildings differing in geometry and height subjected to seismic activities (even repeated ones) in high-risk areas where seismic planning has long been implemented (Goel and Chobra, 1997; Hong and Hwang, 2000; Balkaya and Kalkan, 2003). There has been no research of the latter type in Italy.

Interest in the Global Positioning System (GPS) has increased in recent years, particularly in regard to the precise point positioning (PPP) technique due to its ability to generate accurate instantaneous positioning (Yigit and Gurlek, 2017; Yigit, 2016; Bhagat and Wijeyewickrema, 2017) to detect the dynamic characteristics of structures (Breuer *et al.*, 2015; Ting *et al.*, 2013a; Moschas and Stiros, 2013), especially suspension bridges (Moschas and Stiros, 2011; Ting *et al.*, 2010a, 2010b and 2009; Schaal and Larocca, 2009; Abey *et al.*, 2017; Bayat *et al.*, 2017;). Nonetheless, there have been few applications in the monitoring of buildings.

Correspondence to: Marco Gatti, Department of Engineering, University of Ferrara, via Saragat 1, Ferrara 44123, Italy
  Tel: +393288606252
  E-mail: marco.gatti@unife.it
[†]Professor

During the earthquake in Emilia (Italy) of 2012, ca. 30 permanent GPS stations (Fig. 1) were in operation within a radius of about 100 km from the epicenter, each equipped with an antenna rigidly fixed to the host building and sampling the GPS signal at a high rate.

From the instantaneous displacements derived from the recording of the GPS measurements, it was possible to infer the waveforms produced by the tremors, waveforms treated in the same way as classic seismograms (Kobori *et al.*, 2015; Psimoulis *et al.*, 2015; Moschas *et al.*, 2014; Avallone *et al.*, 2012).

The building hosting the permanent GPS station (the antenna is assumed to be part of the building since it is rigidly fixed to one of the two walls either with steel brackets or directly to the roof with a purposely built reinforced concrete structure) was considered to be an elastic oscillator damped to a single degree of freedom (SDOF), and the instantaneous displacements s(t) in the North-South and East-West directions of the phase centers of the single GPS antennas at each permanent station during the most important seismic sequences (20 May 2012 02:03:53 UTC M_L 5.9; 29 May 2012 07:00:03 UTC M_L 5.8) were calculated in kinematic mode. Subsequently, for each of the two displacements considered as two distinct external forces, the elastic response spectra of the building were determined and from them, the two periods of vibration T along two orthogonal directions coinciding with the walls of the building were extracted.

In this sample, the GPS stations were located in class III buildings (NTC, 2008) such as schools, universities, etc., almost always built before the application of anti-seismic regulations and for which no repair or seismic retrofit interventions had been carried out before the date of the earthquake: during the 2012 earthquake, they did not suffer deformations or failures sufficient to compromise their elastic functionality and thus it was assumed that the building materials did not exceed the linear elastic limit following the seismic ground movements.

These buildings were rapidly surveyed by teams of surveyors to acquire the following information to obtain indirect confirmation of the reliability of the estimated values:
- year of construction;
- building use class;
- if the building was isolated or attached;
- prevalent vertical and horizontal structural type;
- direction of the floor joists;
- number of floors;
- height;
- planimetric dimensions;
- geographical orientation;
- planimetric regularity;
- height regularity;
- presence of stairwells/lift shafts;
- distribution of loads and masses;
- damage and deformations caused by the tremors;
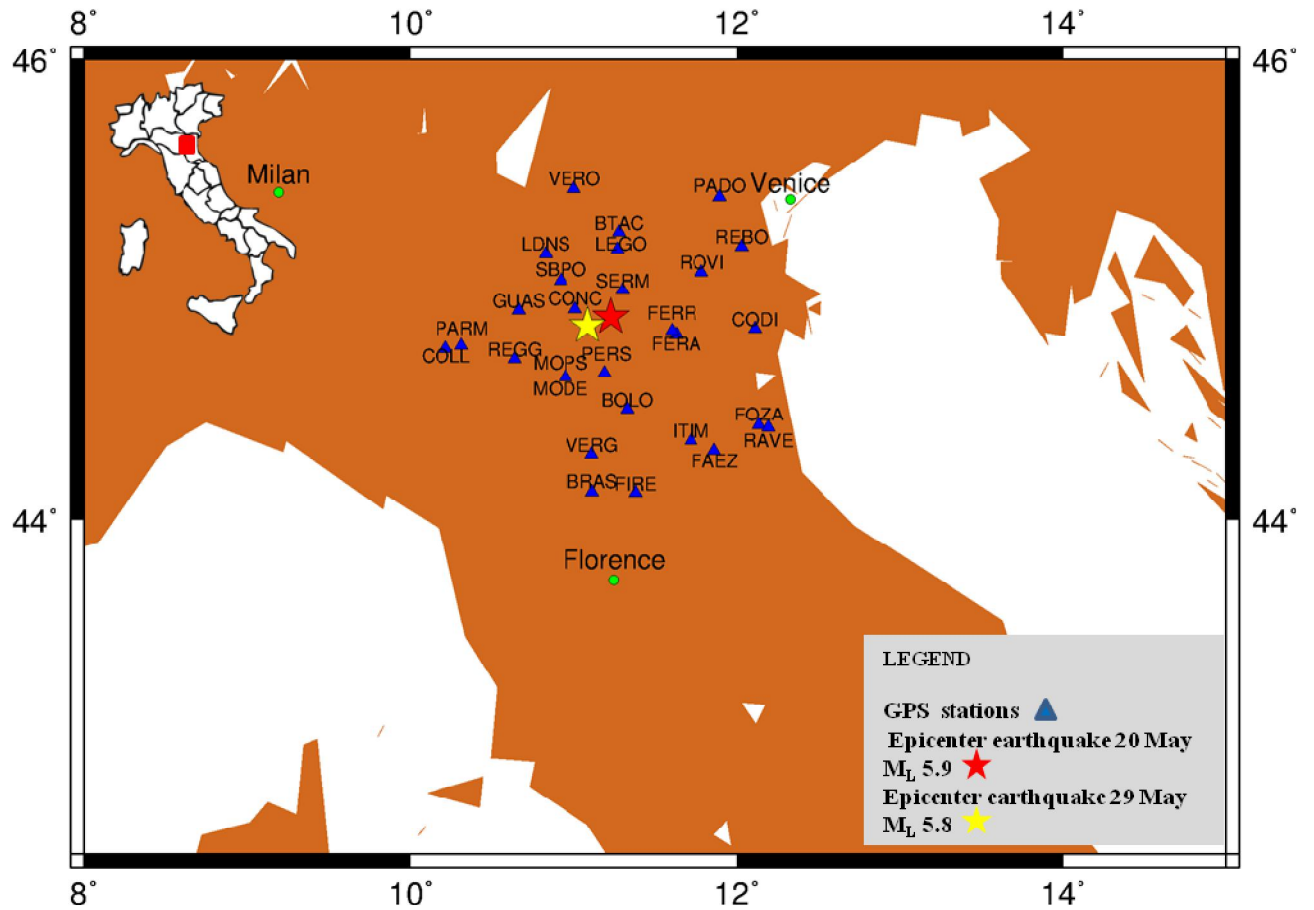- presence or not of repair or seismic retrofit interventions.

Fig. 1 GPS stations and epicenters of the earthquakes of 20 and 29 May 2012, M_L 5.9 and M_L 5.8

In this way, a sufficiently large sample was obtained per building type, geometry (square, rectangular, regular or irregular planimetry), height (from a minimum of 4 to a maximum of 20 m), materials (masonry, reinforced concrete, etc.).

Subsequently, the experimentally obtained periods of vibration were compared with those inferable from the technical literature. The work is divided as follows:

-   an introductory discussion of the simplified numerical relations for calculation of the period of vibration T proposed in the literature, the earthquake in Emilia (Italy) and the permanent GPS stations;
-   a description of the manner of processing the GPS measurements in kinematic mode and calculating the response spectra and periods of vibration T;
-   a summary of the structural geometrical survey of each building and a tabular summary with the geometric and structural characteristics;
-   a comparison between the experimentally estimated values and those proposed in the literature.

2 Simplified numerical relations

The simplified formulation traditionally adopted in the technical literature relates the period of vibration to the height H of the building in the following form:

$$T = \alpha\, H^{\beta} \tag{1}$$

where α is a coefficient dependent on the structural type. The relation is obtained numerically by the Rayleigh method as indicated by Chopra (1995). It appears in ATC3-06 (1978) with $\beta = 0.75$ while the coefficient α, calibrated on the basis of the periods measured during the San Fernando earthquake 1971, is set at 0.025 (if H is in feet) or at 0.06 (if H is expressed in meters). Only later, on the indication of the SEAOC-88 (1988) commentary, the value of α was changed to 0.030 (with H in feet) or 0.073 (with H in meters) and used by the principal regulatory codes. This expression was also adopted by the European EC8

regulations (CEN, 2004) with the rounding off of α to 0.075. It should be emphasized that for use of the preceding determinations it is not necessary to estimate H with precision.

Alternatively, the NEHRP-94 (1994) indications use a relation of the period depending on the number of floors N:

$$T = 0.1 \, N \tag{2}$$

limiting it to buildings with a maximum of 12 floors and inter-floor heights not less than 3 m. This formulation was frequently employed by many regulatory codes before the adoption of Eq. (l).

In the last decade, calibration of coefficients α and β was carried out on an experimental database. In this sense, Goel and Chopra (1997) put together an experimental database of 37 reinforced concrete buildings, seismically designed and of variable height between 10 and 100 m. For each building, they used accelerometers to measure the periods along the transverse and longitudinal planimetric directions. The buildings were subjected to eight Californian earthquakes, from San Fernando in 1971 to Northridge in 1994, of different magnitude and with variable ground accelerations. On the basis of their study, the authors proposed 0.052 for α and 0.9 for β (H in meters).

Similarly Hong and Hwang (2000) proposed α = 0.029 and β = 0.804 (with H in meters) on the basis of the results recorded in 21 seismically designed reinforced concrete buildings in Chinese Taipei subjected to four moderate events which did not violate the elastic behavior of the structure.

It is interesting that the experimental formulations of Goel and Chopra (1997) and Hong and Hwang (2000) provide periods significantly different from each other. This can be attributed to the different seismic design criteria as well as the different construction practices of the two countries.

Finally, it should be mentioned that the Italian regulations differentiate coefficient α according to the materials: values of 0.075 and 0.05 are foreseen for steel buildings and masonry ones, respectively (NTC, 2008).

3 Brief summary of the Emilia earthquake in 2012

The earthquake in Emilia, Lombardy and Veneto (Italy) in 2012 was a seismic event characterized by localized tremors in the Emilian part of the Po Valley, mainly in the provinces of Modena (MO), Ferrara (FE), Mantua (MN), Reggio Emilia (RE), Bologna (Bo) and Rovigo (RO).

The main tremor on 20 May 2012 was felt at 02:03:52 UTC with a duration of 20 s. The epicenter was in the municipal area of Finale Emilia (MO) at a depth of 6.3 km and with an intensity of magnitude 5.9. The accelerations recorded at the nearby seismic station of Mirandola (MO) had a peak horizontal acceleration of 0.264 g in the N-S direction and 0.261 g in the E-W direction. The main tremor of 29 May 2012 occurred at 07:00:03 UTC and lasted 30 s. The epicenter was in the zone between Mirandola (MO), Medolla (MO) and San Felice sul Panaro (MO) at a depth of 9.6 km and with an intensity of magnitude 5.8. The greatest accelerations were recorded at the nearby seismic stations of Mirandola (MO) and Moglia (MN) with a peak horizontal acceleration of 0.296 g (Pontrelli *at al.*, 2012; Scognamiglio *et al.*, 2012).

The earthquake caused severe damage to rural and industrial buildings, historical monuments and older urban buildings. Most of the monuments and places of artistic interest located around the areas of the twomain epicenters suffered serious damage or partial collapse. In some cases, newly built residential buildings were also damaged; this damage was associated with widespread incidents of soil liquefaction (Alessio *et al.*, 2013) situated near abandoned channels of the rivers Secchia, Panaro, Reno and Po, in a broad area between the western sector of the Ferrara province and the present course of the Secchia. Of particular importance was the damage to industrial buildings, all similar to each other, caused by the ineffective construction methods adopted prior to the anti-seismic regulations of 1984 (Bournas *et al.*, 2014). In fact, these prefabricated buildings were constructed in reinforced concrete with horizontal elements simply resting on supports, for which resistance to horizontal translations was provided only by friction. Unfortunately this resulted in the highest percentage of deaths.

4 Permanent GPS stations

Permanent GPS stations were set up in the mid-1990s by consortiums of universities and research organizations (Gurtner, 1995), initially for the sole purpose of tracking GPS satellites (determining their ephemerides) through daily recordings. An antenna, which receives the GPS signal, is rigidly fixed to the structure of a building at its highest point (fixed apparatuses with high electronic performances called

"choke ring" antennas). The antenna is connected to a receiver of similar performance (dual frequency geodetic receiver) located inside the building in a dedicated environment with power lines, data lines (LAN) and supplementary power supply units; the receiver is interfaced with a desktop computer with software for planning and storage of the measurements. An example of the permanent GPS station components are shown in Fig. 2.
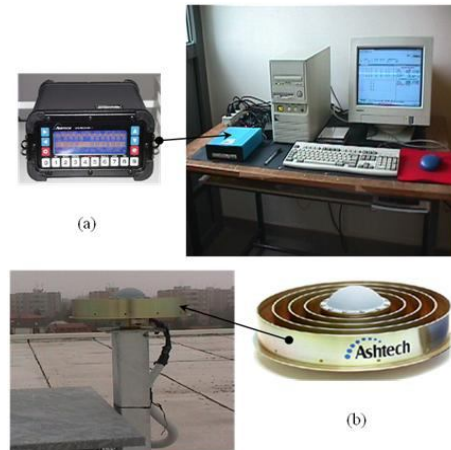

Fig. 2 (a) GPS station in the laboratory; (b) Antenna on the roof

After the first applications, the collected data were shared in international scientific circles for the development of scientific and research activities in the field of geodesy and satellites, such as the correct definition of geodetic reference systems or geodynamic studies aimed at determining movements of the Earth's crust (Wang, 2011). Recently GPS stations have been exploited with master/virtual reference stations in RTKS (Real Time Kinematics Survey) for traditional surveying and mapping. At present, there are networks of GPS stations in almost all the Italian regions, operated by public or private entities: services of positioning in real time and/or in post-processing are provided for a fee or for free.

Twenty-eight permanent GPS stations were used for the present study. They are from 10 to 90 km from the epicenters of the two main seismic events. The GPS measurements from these stations were memorized hourly with a sampling rate between 5 and 20 Hz, in accordance with other authors (Moschas and Stiros, 2015a and 2015b; Ting *et al.*, 2013b; Li *et al.*, 2006).

5 Experimental estimation of the period of vibration

5.1 Processing of the GPS measurements

From the data of the permanent stations, the hourly files recorded during the following seismic events were isolated (identification of the hourly file including the time of the seismic event was carried out with simple editing codes from the files containing the GPS measurements):

- 20 May 2012 02:03:53 UTC M_L 5.9
- 20 May 2012 13:18:02 UTC M_L 5.1
- 29 May 2012 07:00:03 UTC M_L 5.8
- 3 June 2012 19:20:23 UTC M_L 5.1

However, the instantaneous displacements used to derive the response spectra (discussed in the next section) are relative to the two events of highest magnitude.

The GPS measurements consist of phase measurements and code measurements: they represent the input of the calculation model known in the literature as the Precise Point Positioning model - PPP (Zumberge *et al.*, 1997; Bertiger *et al.*, 2010). There are various scientific codes that resolve the PPP model: BERNESE (http://www.bernese.unibe.ch), GAMIT (http://www-gpsg.mit.edu/simon/gtgk), GIPSY (http://gipsy.jpl.nasa.gov/orms/goa), Coulomb US Geological Survey.

For this study, GIPSY OASIS II developed by the Jet Propulsion Laboratory (JPL) was used as single-receiver ambiguity resolution in kinematic positioning (function of time) or PPP (Webb and Zumberge, 1996; Ting *et al.*, 2013c, 2012 and 2011), RINEX 2.11 input file format, measurement types: dual frequency P code and phase; JPL's precise orbit and clock products in the ITRF08 reference system, cutoff

5°, average PDOP less than 2, IGS standards satellite antenna phase center offset, antenna type in RINEX input file, Tropospheric gradients (Bar-Sever *et al.*, 1997) and Second order ionospheric delay (Kedar *et al.*, 2003).

The output of the least squares solution of this model consists of the instantaneous coordinates of the phase center of the antenna in ECEF ITRF08. For convenience, they were expressed in the North-East local system whose origin coincides with the antenna's phase center and the axes coordinated, respectively, with the directions tangent to the meridian and to the parallel passing through the origin. In this way, the instantaneous coordinates subsequent to time t = 0 represent the instantaneous displacements of the antenna, i.e. the vibrations of the building to which it is rigidly fixed: based on the literature they can be considered affected by an error of 0.5 cm/s (Psimoulis *et al.*, 2008). For a considerable number of the stations, it was necessary to rotate the North and East instantaneous coordinates along the directions parallel to the building's external walls: the alignment was achieved with a simple rotation equal to the directional angle of one wall with respect to true North. The directional angles of each station are shown in Table 3, column 9. Finally the coordinates-instantaneous displacements were reduced to zero mean: the latter version represented the external force for calculation of the response spectra (discussed in the next section). By way of example, Fig. 3 reports the coordinates-instantaneous displacements of the permanent station of Concordia (CONC), reduced to zero mean, along the transverse and longitudinal walls following the seismic event of 29 May 07:00:03 UTC. By convention, the shorter walls of the building containing the permanent GPS station were indicated as transverse and the longer ones as longitudinal.
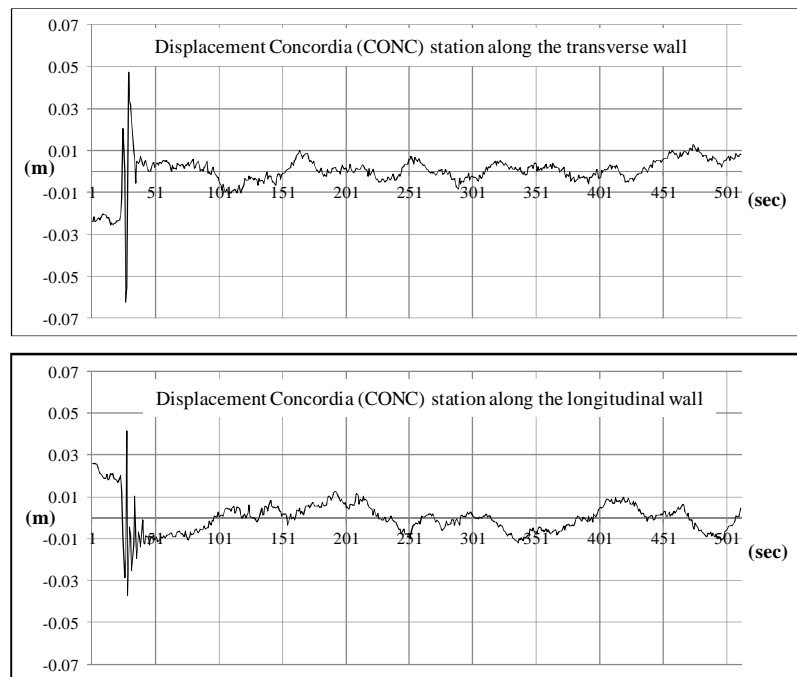

Fig. 3 Displacements (in m) along the (a) transverse and (b) longitudinal walls of the Concordia (CONC) station following the earthquake of 29 May 07:00:03 UTC M_L 5.8

The calculation was performed for all the stations listed in Fig. 1. Figure 4 reports the peak displacement values for each of the two walls following the two seismic events: the vector centers coincide with the position of the GPS antenna and its orientation along the transverse and longitudinal walls.

5.2 Calculation of the response spectra and extraction of the periods of vibration T

As the single building hosting the permanent GPS station was considered to be an elastic oscillator damped to a single degree of freedom (Chopra, 1995) subjected to the external forces numerically defined in the previous section, numerical calculations were carried out in the frequency domain. First, the Fourier transform of the external forces was performed, reducing the instantaneous displacements s(t) from 3600 to 512 s (the latter extracted around the peak displacement), and then their ratio was determined with the transfer function of the oscillator: the latter is represented by a complex number that depends on the sampling frequency of the GPS measurements, the unknown period T and the damping. Setting a damping value of 0.05 and a T value, the maximum value of the ratio was extracted at different frequencies. Extraction of the maximum value was carried out n times, each time increasing T by 0.01 s, up to a total of

3. The curve obtained by plotting the T values from zero to three on the abscissa and the corresponding maximums (amplitudes) on the ordinate is the response spectrum in displacement (or in pseudo-velocity and pseudo-acceleration).

Fig. 4 Peak displacements measured along the walls of the permanent stations following the seismic events of 20 May 2:03:53 UTC M$_L$ 5.9 and 29 May 7:00:03 UTC M$_L$ 5.8

By way of example, Fig. 5 shows the plots of the response spectra of displacement along the transverse and longitudinal walls of the Concordia (CONC) station, obtained from the respective displacements shown in Fig. 3. The maximum amplitude of the spectrum calculated along the transverse wall was 6.5 cm, corresponding to a period of vibration in the same direction of 0.31 s; the maximum amplitude of the spectrum calculated along the longitudinal wall was 4.1 cm, corresponding to a period of

vibration of 0.21 s. The period of vibration T was estimated with an error equal to the fixed increment. For this calculation, a dedicated code was developed in the Matlab environment.

Fig. 5 Response spectra of displacements along the (a) transverse and (b) longitudinal walls of the Concordia (CONC) station following the earthquake of 29 May 07:00:03 UTC M_L 5.8

The numerical calculation was performed for all the buildings hosting the GPS stations reported in Fig. 1. The results are reported in Table 1.
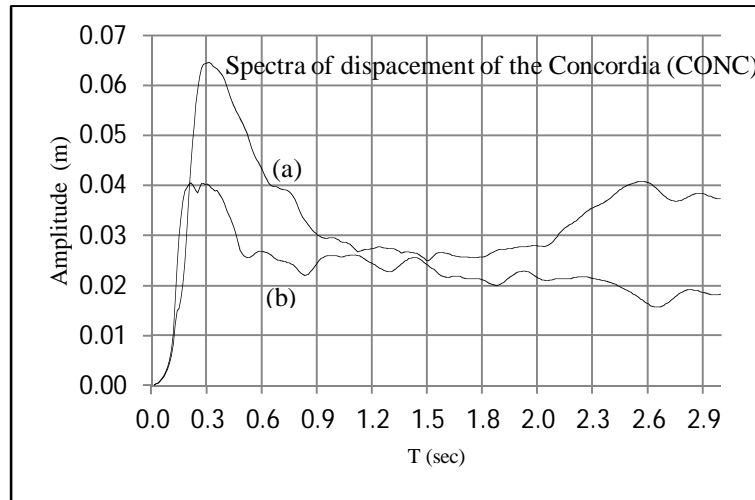
Table 1 Periods of vibration (in seconds) and respective maximum amplitudes calculated for each of the permanent stations during the seismic events of 20 May 2:03:53 UTC M_L 5.9 and 7:00:03 UTC M_L 5.8

Name	Date of the seismic event	Direction of displacement/vibration	Response spectrum	
			T (s)	Amplitude (cm)
Faenza (FAEZ)	20/05/2012	Axes walls transverse	0.45	3.5
		Parallel axes walls longitudinal	0.32	2.4
	29/05/2012	Axes walls transverse	0.42	1.0
		Parallel axes walls longitudinal	0.32	0.7
Ravenna (RAVE)	20/05/2012	Parallel axes walls north-east	0.29	2.0
		Parallel axes walls south-east	0.26	1.8
Bologna (BOLO)	20/05/2012	Parallel axes walls transverse	0.54	3.3
		Parallel axes walls longitudinal	0.58	3.7
Ferrara (FERA)	20/05/2012	Axes walls longitudinal	0.4	6.6
		Parallel axes walls transverse	0.27	3.4
	29/05/2016	Axes walls longitudinal	0.44	0.9
		Parallel axes walls transverse	0.25	0.8
Codigoro (CODI)	20/05/2012	Parallel axes walls north-south	0.19	2.3
		Parallel axes walls east-west	0.16	0.6
	29/05/2012	Parallel axes walls north-south	0.2	0.5
		Parallel axes walls east-west	0.15	0.4
Imola (ITIM)	20/05/2012	Parallel axes walls north-south	0.5	3.6
		Parallel axes walls east-west	0.51	3.9
Collecchio (COLL)	20/05/2012	Parallel axes walls transverse	0.54	0.6
		Parallel axes walls longitudinal	0.42	0.7
	29/05/2012	Parallel axes walls transverse	0.53	0.4
		Parallel axes walls longitudinal	0.46	0.5
Concordia (CONC)	29/05/2012	Parallel axes walls transverse	0.31	6.5
		Axes walls longitudinal	0.21	4.1
Ferrara (FERR)	20/05/2012	Axes walls transverse	0.35	9.2
		Parallel axes walls longitudinal	0.39	8.5
	29/05/2012	Axes walls transverse	0.33	1.0
		Parallel axes walls longitudinal	0.39	1.0
Guastalla (GUAS)	20/05/2012	Axes walls longitudinal	0.18	0.7
		Parallel axes walls transverse	0.33	1.5
	29/05/2012	Axes walls longitudinal	0.16	0.6
		Parallel axes walls transverse	0.3	1.2

Reggio Emilia (REGG)	20/05/2012	Parallel axes walls transverse	0.31	1.2
		Parallel axes walls longitudinal	0.26	1.4
	29/05/2012	Parallel axes walls transverse	0.27	0.9
		Parallel axes walls longitudinal	0.28	0.8
San Giovanni in Persiceto (PERS)	20/05/2012	Parallel axes walls north-east	0.43	8.1
		Parallel axes walls south-east	0.31	5.5
	29/05/2012	Parallel axes walls north-east	0.42	7.0
		Parallel axes walls south-east	0.315	4.7
Vergato (VERG)	20/05/2012	Parallel axes walls transverse	0.15	0.5
		Parallel axes walls longitudinal	0.29	1.1
	29/05/2012	Parallel axes walls transverse	0.16	0.5
		Parallel axes walls longitudinal	0.29	0.8
Ravenna (FOZA)	20/05/2012	Parallel axes walls transverse	0.16	1.0
		Parallel axes walls longitudinal	0.17	1.6
	29/05/2012	Parallel axes walls transverse	0.16	0.4
		Parallel axes walls longitudinal	0.16	0.4
Rebosola (REBO)	20/05/2012	Parallel axes walls north-south	0.43	3.0
		Axes walls east-west	0.51	2.3
	29/05/2012	Parallel axes walls north-south	0.48	1.2
		Axes walls east-west	0.54	1.0
Sermide (SERM)	20/05/2012	Axes walls longitudinal north-south	0.31	6.1
		Parallel axes walls transverse east-west	0.31	3.4
	29/05/2012	Axes walls longitudinal north-south	0.34	5.5
		Parallel axes walls transverse east-west	0.34	3.3
Verona (VERO)	20/05/2012	Axes walls longitudinal	0.58	0.7
		Axes walls transverse	0.55	0.6
	29/05/2012	Axes walls longitudinal	0.56	0.7
		Axes walls transverse	0.52	0.4
Firenzuola (FIRE)	20/05/2012	Parallel axes walls transverse	0.35	0.6
		Parallel axes walls longitudinal	0.385	1.3
	29/05/2012	Parallel axes walls transverse	0.36	0.4
		Parallel axes walls longitudinal	0.37	0.6
Brasimone (BRAS)	20/05/2012	Parallel axes walls transverse	0.33	0.7
		Axes walls longitudinal	0.23	0.3
	29/05/2012	Parallel axes walls transverse	0.3	0.6
		Axes walls longitudinal	0.25	0.4
Modena (MODE)	20/05/2012	Parallel axes walls transverse	0.34	3.6
		Parallel axes walls longitudinal	0.28	1.9
	29/05/2012	Parallel axes walls transverse	0.32	3.9
		Parallel axes walls longitudinal	0.31	1.3
Parma (PARM)	20/05/2012	Parallel axes walls transverse	0.29	0.5
		Parallel axes walls longitudinal	0.29	0.6
	20/05/2012	Parallel axes walls transverse	0.3	0.6
		Parallel axes walls longitudinal	0.3	0.5
San Benedetto Po (SBPO)	20/05/2012	Axes walls north-south	0.3	4.0
		Axes walls east-west	0.35	4.5
	29/05/2012	Axes walls north-south	0.37	4.3
		Axes walls east-west	0.28	2.4
Legnago (LEGO)	20/05/2012	Parallel axes walls north-south	0.33	3.9
		Axes walls east-west	0.18	0.9
	29/05/2012	Parallel axes walls north-south	0.36	4.6
		Axes walls east-west	0.2	0.9
Mantova (LDNS)	20/05/2012	Axes walls transverse	0.31	2.9
		Axes walls longitudinal	0.34	3.0
	29/05/2012	Axes walls transverse	0.3	1.6
		Axes walls longitudinal	0.3	1.9
Padova (PADO)	20/05/2012	Axes walls transverse	0.33	1.2
		Axes walls longitudinal	0.45	1.3
	29/05/2012	Axes walls transverse	0.37	0.5
		Axes walls longitudinal	0.44	0.6
Rovigo (ROVI)	20/05/2012	Parallel axes walls north-south	0.42	5.2
		Parallel axes walls east-west	0.37	2.7
	29/05/2012	Parallel axes walls north-south	0.39	1.6
		Parallel axes walls east-west	0.33	1.5

Verona (BTAC)	20/05/2012	Parallel axes walls north-south	0.33	2.0
		Parallel axes walls east-west	0.38	1.6
	29/05/2012	Parallel axes walls north-south	0.35	2.9
		Parallel axes walls east-west	0.36	1.8
Modena (MOPS)	20/05/2012	Parallel axes walls transverse	0.34	3.6
		Parallel axes walls longitudinal	0.34	2.1
	29/05/2012	Parallel axes walls transverse	0.32	3.7
		Parallel axes walls longitudinal	0.32	1.5

For buildings in which there were temporal displacements recorded for multiple seismic events, i.e. for which there was more than a single estimate of the period of vibration T, a weighted mean value with weight equal to the maximum amplitude value was attributed. The results are summarized in Table 2.

Table 2 Mean periods of vibrations (in seconds) calculated for each of the permanent stations as a weighted mean of the inferred values during the two seismic events of 20 May 2:03:53 UTC M_L 5.9 and 7:00:03 UTC M_L 5.8

Name	Direction displacement/vibration	$T_m(s)$
Faenza (FAEZ)	Axes walls transverse	0.44
	Parallel axes walls longitudinal	0.32
Ravenna (RAVE)	Parallel axes walls north-east	0.29
	Parallel axes walls south-east	0.26
Bologna (BOLO)	Parallel axes walls transverse	0.54
	Parallel axes walls longitudinal	0.58
Ferrara (FERA)	Axes walls longitudinal	0.40
	Parallel axes walls transverse	0.27
Codigoro (CODI)	Parallel axes walls north-south	0.19
	Parallel axes walls east-west	0.16
Imola (ITIM)	Parallel axes walls north-south	0.50
	Parallel axes walls east-west	0.51
Collecchio (COLL)	Parallel axes walls transverse	0.54
	Parallel axes walls longitudinal	0.44
Concordia (CONC)	Parallel axes walls transverse	0.31
	Axes walls longitudinal	0.21
Ferrara (FERR)	Axes walls transverse	0.35
	Parallel axes walls longitudinal	0.39
Guastalla (GUAS)	Axes walls longitudinal	0.17
	Parallel axes walls transverse	0.32
Reggio Emilia (REGG)	Parallel axes walls transverse	0.29
	Parallel axes walls longitudinal	0.27
San Giovanni in Persiceto (PERS)	Parallel axes walls north-east	0.43
	Parallel axes walls south-east	0.31
Vergato (VERG)	Parallel axes walls transverse	0.16
	Parallel axes walls longitudinal	0.29
Ravenna (FOZA)	Parallel axes walls transverse	0.16
	Parallel axes walls longitudinal	0.17
Rebosola (REBO)	Parallel axes walls north-south	0.44
	Axes walls east-west	0.52
Sermide (SERM)	Axes walls longitudinal north-south	0.31
	Parallel axes walls transverse east-west	0.31
Verona (VERO)	Axes walls longitudinal	0.57
	Axes walls transverse	0.54
Firenzuola (FIRE)	Parallel axes walls transverse	0.35
	Parallel axes walls longitudinal	0.38
Brasimone (BRAS)	Parallel axes walls transverse	0.32
	Axes walls longitudinal	0.24
Modena (MODE)	Parallel axes walls transverse	0.33
	Parallel axes walls longitudinal	0.29
Parma (PARM)	Parallel axes walls transverse	0.30
	Parallel axes walls longitudinal	0.29
San Benedetto Po (SBPO)	Axes walls north-south	0.34
	Axes walls east-west	0.33
Legnago (LEGO)	Parallel axes walls north-south	0.35

	Axes walls east-west	0.19
Mantova (LDNS)	Axes walls transverse	0.31
	Axes walls longitudinal	0.32
Padova (PADO)	Axes walls transverse	0.34
	Axes walls longitudinal	0.45
Rovigo (ROVI)	Parallel axes walls north-south	0.41
	Parallel axes walls east-west	0.36
Verona (BTAC)	Parallel axes walls north-south	0.34
	Parallel axes walls east-west	0.37
Modena (MOPS)	Parallel axes walls transverse	0.33
	Parallel axes walls longitudinal	0.33

6 Rapid structural geometric survey

The minimal geometric and structural characteristics of the investigated buildings necessary to verify the test results were collected with a rapid survey consisting of an inspection and compilation of a technical-numerical and informational questionnaire. No particularly complex or detailed geometrical surveys were carried out, except for measurement of the height of the building and the linear planimetric dimensions of the external perimeter; on-site inspections or tests of materials were not performed, nor were complex structural modelling.

In this phase, a visual examination was conducted to check for structural or plant failures, repair or seismic retrofit interventions, as well as deformations, failures or relative movements between structural elements at the foundation level induced by the earthquake (Hao *et al.*, 2016).

In particular, the following information was acquired during the survey:
- year of construction;
- building use class;
- if the building was isolated or attached;
- prevalent vertical and horizontal structural type;
- direction of the floor joists;
- number of floors;
- height (prevalent min - max);
- planimetric dimensions (prevalent min - max);
- geographical orientation;
- planimetric regularity;
- height regularity;
- presence of stairwells/lift shafts;
- distribution of loads and masses.

A summary of the survey is given in Table 3. The prevalent structural type is reinforced concrete frame with either concrete or brick vertical infill walls. The joists of the floor assemblies (in hollow-core concrete for the floors or in concrete for the roof) are always arranged parallel to the direction of the shorter planimetric length of the building, almost never staggered; the prevailing roof cover is flat. There are some masonry buildings with floors in hollow-core concrete and pitched roofs. The heights vary from a minimum of 4 to a maximum of 20 m, with a maximum of five floors (inter-floor heights ranging from 3 to 5 m). The prevailing planimetric geometry is rectangular with an equal incidence on both the planimetric and height regularity. In all buildings, except single-story ones, there are stairwells and lift shafts, almost never in a central position, and the distribution of permanent-incidental loads and masses is generally uniform. Finally, up to the date of the earthquakes, there had been no repair or seismic retrofit interventions but only quantitative vulnerability analyses, and most of the buildings had not suffered damage such to render them wholly or partly unusable. The latter finding confirms the hypothesis underlying this study, i.e. that the building materials did not exceed the linear elastic limit following the seismic ground movements.

Table 3 Summary of the information acquired during the rapid survey carried out for each permanent GPS station

Name	Year of construction	Use class - Attached/Isolated	Vertical structural type	Horizontal structural type and direction of the floor joists	No. of floors	Height eaves/top (m)	Principal dimension L1xL2 (m)	Orientation (°) from North	Planimetric regularity	Height regularity	Stairwells/lift shafts	Distribution of loads and masses
Faenza (FAEZ)	1950	II attached	Frame in prestressed reinforced concrete with horizontal elements simply resting on supports and brick infill walls	Concrete floor assemblies. Flat concrete roof. Joists mainly arranged along the shorter side	2	8.8	12.5x65	24°	No	No	Yes	Yes
Ravenna (RAVE)	1975	III attached	Frame in reinforced concrete and brick infill walls	Hollow-core concrete floor assemblies. Flat hollow-core concrete roof. Joists arranged parallel to the transverse direction	2	8.3	9x35	18°	No	No	Yes	Yes
Bologna (BOLO)	1935	III attached	Full masonry	Hollow-core concrete floor assemblies. Flat hollow-core concrete roof. Joists arranged parallel to the transverse direction	4	20	20x40	15°	No	No	Yes	No
Ferrara (FERA)	1990	II attached	Frame in prestressed reinforced concrete with horizontal elements simply resting	Light slab floor assemblies. Flat roof in honeycomb slabs. Joists arranged parallel to the	2	8.7	18x23	60°	Yes	Yes	Yes	Yes

				on supports and brick infill walls	transverse direction								
Codigoro (CODI)	1978	III isolated	Frame in prestressed reinforced concrete with horizontal elements simply resting on supports and multiwall polycarbonate panel infill walls	Reinforced concrete slabs. Joists arranged parallel to the longitudinal direction	Single-story	3.6	75x137	0°	Yes	Yes	No	Yes
Imola (ITIM)	1970	III attached	Frame in reinforced concrete and brick infill walls	Hollow-core concrete floor assemblies. Flat hollow-core concrete roof. Joists arranged parallel and perpendicular to the transverse direction	5	18.54	43x44	0°	No	No	Yes	No
Collecchio (COLL)	1930	III isolated	Full masonry	Hollow-core concrete floor assemblies. Pitched hollow-core concrete roof. Joists arranged parallel and perpendicular to the transverse direction	3	15	18x30	48°	No	No	Yes	Yes
Concordia (CONC)	2008	II isolated	Frame in reinforced concrete with horizontal	Variable-section main beams, and secondary	Single-story	7.10/8.56	17x24	25°	Yes	Yes	No	Yes

				beams. Pitched roof in light slabs								
			elements simply resting on supports and concrete infill walls									
Ferrara (FERR)	1993	III attached	Three-dimensional frame in reinforced concrete and brick infill walls	Hollow-core concrete floor assemblies. Pitched hollow-core concrete roof. Joists arranged parallel to the transverse direction	4	10.2	84x29	37°	No	Yes	Yes	Yes
Guastalla (GUAS)	1970	III attached	Frame in reinforced concrete and brick infill walls	Hollow-core concrete floor assemblies. Flat concrete roof. Joists arranged parallel to the transverse direction	3	9	48x50	18°	No	No	Yes	Yes
Reggio Emilia (REGG)	1980	III attached	Frame in reinforced concrete and brick infill walls	Hollow-core concrete floor assemblies. Flat concrete roof. Joists arranged parallel to the transverse direction	3	15	31x40	59°	No	Yes	Yes	Yes
San Giovanni in Persiceto (PERS)	1996	III attached	Three-dimensional frame in reinforced concrete and brick infill walls	Hollow-core concrete floor assemblies. Mixed (flat/pitched) hollow-core concrete roof. Joists arranged parallel to the transverse	4	16.3	13x32	37°	No	Yes	Yes	Yes

				direction								
Vergato (VERG)	2000	III attached	Three-dimensional frame in reinforced concrete and brick infill walls	Hollow-core concrete floor assemblies. Flat concrete roof. Joists arranged parallel to the transverse direction	2	9	18x20	37°	No	Yes	Yes	Yes
Ravenna (FOZA)	1990	III isolated	Frame in reinforced concrete and concrete infill walls	Concrete floor assemblies. Sloping concrete roof. Joists arranged parallel to the transverse direction	2	6	37x96	59°	Yes	No	Yes	Yes
Rebosola (REBO)	1920	II isolated	Full masonry	Hollow-core concrete floor assemblies. Mixed (flat/pitched) hollow-core concrete roof. Joists arranged parallel to the East-West direction	3	12	6x10	0°	Yes	Yes	No	Yes
Sermide (SERM)	1930	II attached	Full masonry	Hollow-core concrete floor assemblies. Wooden pitched roof. Joists arranged parallel to the transverse direction	3	11.4	4x9	63°	No	Yes	Yes	Yes
Verona (VERO)	1950	II attached	Full masonry	Hollow-core concrete floor assemblies. Pitched hollow-core	5	18	38x45	16°	No	Yes	Yes	Yes

				concrete roof. Joists arranged parallel to the transverse direction								
Firenzuola (FIRE)	1400	II isolated	Regular stonework	Wooden floor assemblies. Flat roof in wood and hollow-core concrete. Joists arranged parallel to the transverse direction	3	20	12x20	68°	No	Yes	Yes	Yes
Brasimone (BRAS)	1980	II isolated	Frame in prestressed reinforced concrete with horizontal elements simply resting on supports and multiwall polycarbonate panel infill walls	Reinforced concrete slabs. Joists arranged parallel to the longitudinal direction	2	6	7x34	35°	Yes	Yes	Yes	Yes
Modena (MODE)	1996	III isolated	Three-dimensional frame in reinforced concrete and brick infill walls	Hollow-core concrete floor assemblies. Flat hollow-core concrete roof. Joists arranged parallel to the transverse direction	3	12	30x67	37°	No	Yes	Yes	Yes
Parma (PARM)	1990	II isolated	Frame in reinforced concrete and concrete infill walls	Concrete floor assemblies. Flat concrete roof. Joists arranged parallel to the	Single-story	6	25x49	36°	Yes	Yes	No	Yes

				transverse direction								
San Benedetto Po (SBPO)	1996	II isolated	Full masonry	Hollow-core concrete floor assemblies. Pitched hollow-core concrete roof. Joists arranged parallel to the East-West direction	2	2.6-4	13x13	0°	No	No	Yes	Yes
Legnago (LEGO)	2000	II isolated	Frame in reinforced concrete and glass infill walls	Concrete floor assemblies. Flat concrete roof. Joists arranged parallel to the East-West direction	3	12.5	10x29	0°	Yes	Yes	Yes	Yes
Mantova (LDNS)	2000	III attached	Frame in reinforced concrete and glass infill walls	Concrete floor assemblies. Flat concrete roof. Joists arranged parallel to the transverse direction	3	13.5	153x163	66°	No	Yes	Yes	Yes
Padova (PADO)	1970	II isolated	Frame in reinforced concrete and brick infill walls	Hollow-core concrete floor assemblies. Flat concrete roof. Joists arranged parallel to the transverse direction	2	7.34	11x112	21°.5	No	Yes	Yes	Yes
Rovigo (ROVI)	2000	II isolated	Frame in reinforced concrete and brick infill walls	Hollow-core concrete floor assemblies. Flat hollow-core concrete roof.	3	12	32x32	0°	Yes	Yes	Yes	Yes

				Staggered joist arrangement								
Verona (BTAC)	1990	II isolated	Full masonry	Hollow-core concrete floor assemblies. Pitched hollow-core concrete roof. Joists arranged parallel to the North-South direction	2	6	11x14	0°	Yes	Yes	Yes	Yes
Modena (MOPS)	1996	III isolated	Three-dimensional frame in reinforced concrete and brick infill walls	Hollow-core concrete floor assemblies. Flat hollow-core concrete roof. Joists arranged parallel to the transverse direction	3	12	27x67	36°	No	Yes	Yes	==Yes==

7 Comparisons

The experimental periods were compared with those inferable from the empirical relations (1) and (2) in section 2, with H set as the height to the building's eaves and n the number of floors above ground. Table 4 reports the values calculated with the empirical relations, while Table 5 reports the comparisons. Since there are two experimental determinations of T (along the transverse and longitudinal walls of the building), homogeneous comparisons were made by extrapolating a single experimental value of T equal to the mean of the transverse and longitudinal spectra.

Table 4 Calculation of the periods by means of the relations (1) and (2) reported in the technical literature. (°) Height to the eaves. (*) Above ground. (°°) $T = \alpha H^{\beta}$ with $\alpha = 0.075$ for reinforced concrete buildings and 0.05 for masonry buildings, $\beta = 0.75$. (°°°) $T = 0.1 N$

Name	Height (m) (°)	No. floors (*)	T (s) (°°)	T (s) (°°°)
Faenza (FAEZ)	8.8	2	0.38	0.20
Ravenna (RAVE)	8.3	2	0.37	0.20
Bologna (BOLO)	20.0	4	0.47	0.40
Ferrara (FERA)	8.7	2	0.38	0.20
Codigoro (CODI)	3.6	1	0.20	0.10
Imola (ITIM)	18.54	5	0.67	0.50
Collecchio (COLL)	15	3	0.38	0.30
Concordia (CONC)	7.1	1	0.33	0.10
Ferrara (FERR)	11.1	3	0.46	0.30
Guastalla (GUAS)	9	3	0.39	0.30
Reggio Emilia (REGG)	15	3	0.57	0.30
San Giovanni in Persiceto (PERS)	15.3	4	0.58	0.40
Vergato (VERG)	9	2	0.39	0.20
Ravenna (FOZA)	6	2	0.29	0.20
Rebosola (REBO)	12	3	0.32	0.30
Sermide (SERM)	11.4	3	0.31	0.30
Verona (VERO)	18	5	0.44	0.50
Firenzuola (FIRE)	20	3	0.47	0.30
Brasimone (BRAS)	6	2	0.29	0.20
Modena (MODE)	12.03	4	0.48	0.40
Parma (PARM)	6	1	0.29	0.10
San Benedetto Po (SBPO)	4.6	2	0.16	0.20
Legnago (LEGO)	12.5	3	0.50	0.30
Mantova (LDNS)	13.5	3	0.53	0.30
Padova (PADO)	7.34	2	0.33	0.20
Rovigo (ROVI)	16.33	4	0.61	0.40
Verona (BTAC)	6	2	0.19	0.20
Modena (MOPS)	12.05	4	0.49	0.40

Table 5 Comparisons of the experimentally estimated values and those based on the relations (1) and (2) reported in the technical literature. (°°) $T = \alpha H^{\beta}$ with $\alpha = 0.075$ for reinforced concrete buildings and 0.05 for masonry buildings, $\beta = 0.75$. (°°°) $T = 0.1 N$

Name	T (s) (°°)	T (s) (°°°)	T_m (s)
Faenza (FAEZ)	0.38	0.20	0.38
Ravenna (RAVE)	0.37	0.20	0.28
Bologna (BOLO)	0.47	0.40	0.57
Ferrara (FERA)	0.38	0.20	0.34
Codigoro (CODI)	0.20	0.10	0.17
Imola (ITIM)	0.67	0.50	0.51
Collecchio (COLL)	0.38	0.30	0.54
Concordia (CONC)	0.33	0.10	0.26
Ferrara (FERR)	0.46	0.30	0.37
Guastalla (GUAS)	0.39	0.30	0.24
Reggio Emilia (REGG)	0.57	0.30	0.28
San Giovanni in Persiceto	0.58	0.40	0.37
Vergato (VERG)	0.39	0.20	0.22
Ravenna (FOZA)	0.29	0.20	0.16
Rebosola (REBO)	0.32	0.30	0.45
Sermide (SERM)	0.31	0.30	0.31
Verona (VERO)	0.44	0.50	0.55

Firenzuola (FIRE)	0.47	0.30	0.37
Brasimone (BRAS)	0.29	0.20	0.28
Modena (MODE)	0.48	0.40	0.31
Parma (PARM)	0.29	0.10	0.29
San Benedetto Po (SBPO)	0.16	0.20	0.33
Legnago (LEGO)	0.50	0.30	0.35
Mantova (LDNS)	0.53	0.30	0.32
Padova (PADO)	0.33	0.20	0.39
Rovigo (ROVI)	0.61	0.40	0.38
Verona (BTAC)	0.19	0.20	0.35
Modena (MOPS)	0.49	0.40	0.33

Table 6 reports the mean, standard deviation and min/max differences between the periods T obtained using the empirical relations (1) and (2) reported in the literature and the experimentally estimated periods.

Table 6 Means, standard deviations and min/max differences. (°°) T = α H $^\beta$ with α = 0.075 for reinforced concrete buildings and 0.05 for masonry buildings, β = 0.75. (°°°) T = 0.1 N

	δT (°°)	δT (°°°)
Mean (s)	0.06	-0.07
Standard deviation (s)	0.13	0.09
Difference max (s)	0.29	0.09
Difference min (s)	-0.17	-0.24

Finally, on the assumption that buildings constructed after 1984 (the year of the first important Italian technical regulations governing seismic constructions, D.M. 19 Giugno 1984 "Norme tecniche relative alle costruzioni sismiche") were designed to withstand vertical and horizontal forces, that three-dimensional frames were more constrained than one-dimensional ones and that reinforced concrete was a more elastic material than masonry, the periods obtained from relation (1) were compared with the experimentally estimated periods according to the year of construction (buildings constructed before and after 1984), the structural type (buildings with one-, two- and three-dimensional frames) and the building material (reinforced concrete and masonry buildings). The comparisons are reported in Figs. 6, 7 and 8.
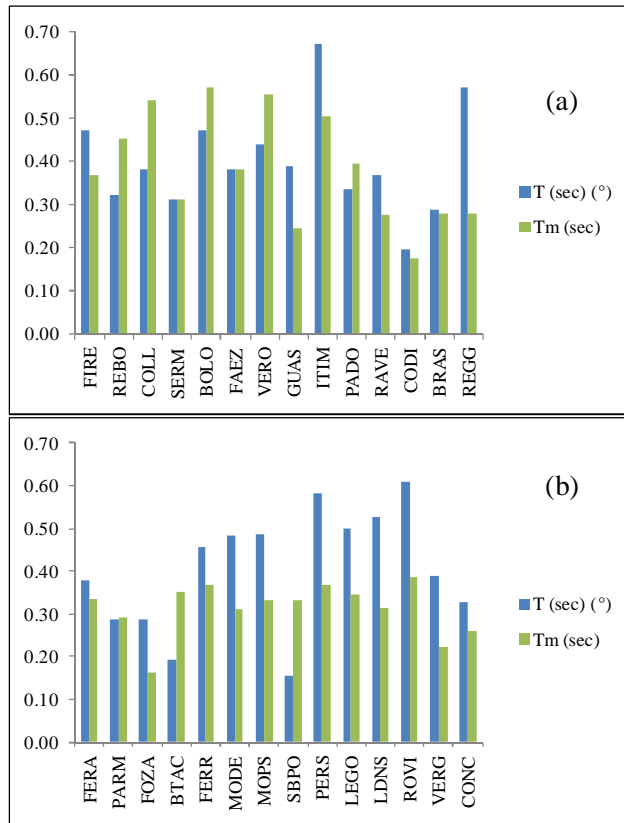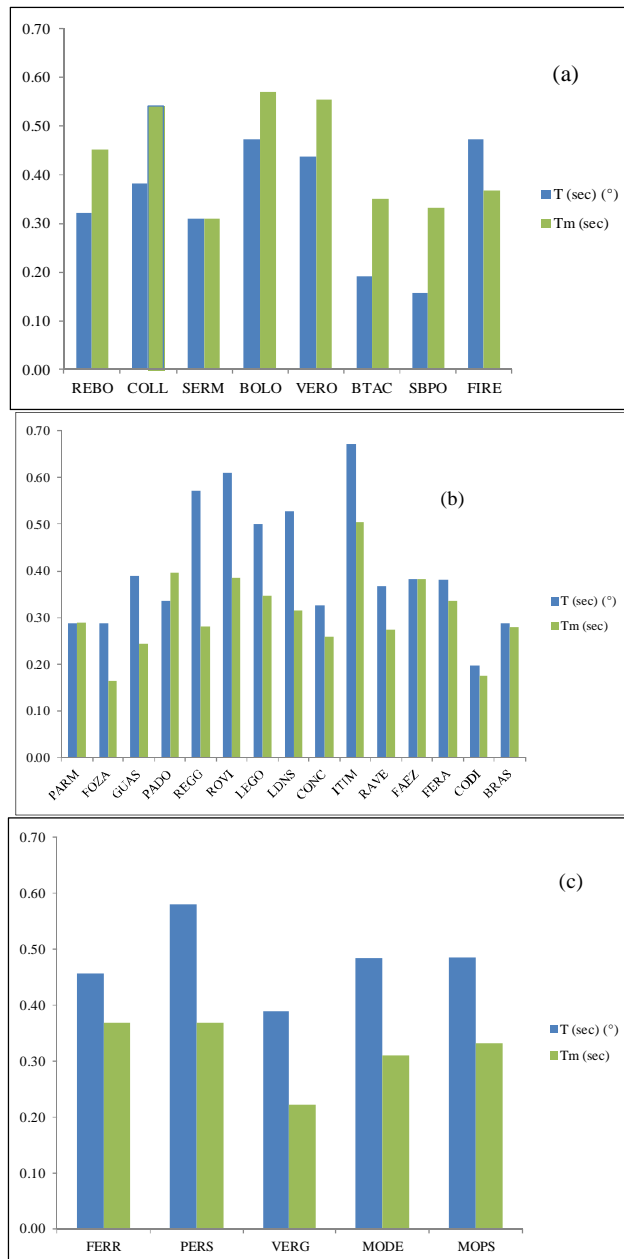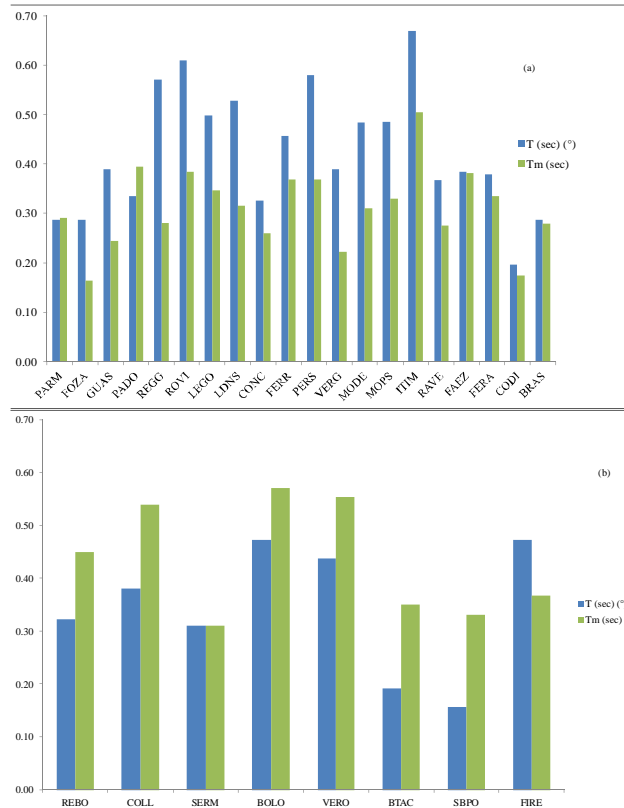
Fig. 6 Comparisons of the experimentally estimated values and those based on the relation (1) reported in the technical literature according to year of construction: (a) before 1984 and (b) after 1984. (°) $T = \alpha H^{\beta}$ with $\alpha = 0.075$ for reinforced concrete buildings and 0.05 for masonry buildings, $\beta = 0.75$

Fig. 7 Comparisons of the experimentally estimated values and those based on the relation (1) reported in the technical literature according to the structural type: buildings with (a) one-, (b) two- and (c) three-dimensional frames. (°) $T = \alpha H^{\beta}$ with $\alpha = 0.075$ for reinforced concrete buildings and 0.05 for masonry buildings, $\beta = 0.75$

Fig. 8 Comparisons of the experimentally estimated values and those based on the relation (1) reported in the technical literature according to the building material: (a) reinforced concrete and (b) masonry. (°) $T = \alpha\, H^{\beta}$ with $\alpha = 0.075$ for reinforced concrete buildings and 0.05 for masonry buildings, $\beta = 0.75$

8 Conclusions

The present study confirmed that GPS is an emerging tool for the monitoring of dynamic displacements in buildings subjected to seismic events. The good possibility of using GPS measurements is due both to the recording capacity (new devices are equipped with boards of up to 100 sampling rates) and to the sensitivity (Table 1 shows that reliable T values were obtained even with small horizontal displacements, ca. 1 cm, recorded in the buildings furthest from the epicenter). Therefore, it may be possible to integrate or replace GPS station networks with accelerometer networks, especially in areas where the former are most deficient.

The results for the estimates of T are as follows:

- for the same building geometry, distribution of masses and type of constraints, the period along one wall is substantially different from that in the orthogonal direction (Table 1); this is because the distribution of stiffnesses never coincides with that of loads, especially for buildings constructed before the anti-seismic regulations were enacted. For this reason, in structural controls of existing buildings, it is incorrect to assume the same value of T for both walls;

- the differences between the values calculated with empirical relation (1) and with relation (2) and the experimentally estimated values are, respectively, lower and higher on average; however, the standard deviation of the mean difference from the value based on relation (2) is lower (Table 6). Therefore, the period/number of floors relation suggested by NEHRP (1994) generally provides more correct results than relation (1) in the range of heights (ca. 3 m) typical of Italian buildings;

- regarding the year of construction (Figs. 6(a) and (b)), in almost all the pre-1984 buildings the value of T obtained from relation (1) is lower than the experimentally estimated value; the opposite holds for post-1984 buildings: this result contradicts the expectation that buildings designed to withstand both gravitational and horizontal loads would have a lower elastic periods;

- for the structural type with one-dimensional frames (typical of masonry buildings with floor joists oriented along the shortest direction), the T value obtained from relation (1) is substantially lower than the experimentally estimated value (Figure 7(a)); the opposite is true for the types with two-dimensional and three-dimensional frames (typical of reinforced concrete structures with beams and pillars, in the former case with joists oriented in the shorter direction, Figure 7(b), and in the latter case with joists oriented

alternately in one or the other direction, Figure 7(c): this result contradicts the theoretical expectation that framed structures would have lower elastic periods;

- only the comparison of building materials is reliable: the T value derived from relation (1) is higher than the experimentally estimated value in the case of reinforced concrete buildings (Figure 8(a)), whereas it is lower in the case of masonry buildings (Figure 8(b)).

At least in theory, it follows that basing calculation of the elastic period T on the period/height relation (1) should be reviewed or at least carefully considered in the choice of coefficients α and β, especially for buildings designed with obsolete seismic specifications or for gravitational loads alone (the overwhelming majority of buildings in Italy).

The limitations of this study lie in the difficulty in choosing a priori the geometry and/or structural type of the building hosting the GPS station.

References

Abey ET, Somasundaran TP, Sajith AS (2017), "Study on seismic performance enhancement in bridges based on factorial analysis," *Earthquake Engineering and Engineering Vibration*, **16**(1): 181–198.

Alessio G, Alfonsi L, Brunori CA, Burrato P, Casula G, Cinti FR, Civico R, Colini L, Cucci L, De Martini PM, Falcucci E, Galadini F, Gaudiosi G, Gori S, Mariucci MT, Montone P, Moro M, Nappi R, Nardi A, Nave R, Pantosti D, Patera A, Pesci A, Pezzo G, Pignone M, Pinzi S, Pucci, Salvi S, Tolomei C, Vannoli P, Venuti A, Villani F (2013), "Liquefaction phenomena associated with the Emilia earthquake sequence of May–June 2012 (Northern Italy)," *Natural Hazards and Earth System Sciences*, **13**: 935-947.

A.T.C. Applied Technological Council (1978), *Tentative provisions for the development of seismic regulations for buildings*, ATC3-06, Applied Technological Council, Palo Alto, California.

Avallone A, D'Anastasio E, Serpelloni E, Latorre D, Cavaliere A, D'Ambrosio C, Del Mese S, Massucci A, Cecere G (2012), "High-rate (1 to 20-Hz) GPS co-seismic dynamic displacements carried out during the 2012 Emilia seismic sequence," *Annals of Geophysics*, **55**(4): 773-779.

Balkaya C, Kalkan E (2003), "Estimation of fundamental periods of shear-wall dominant building structures," *Earthquake Engineering and Structural Dynamics*, **32**: 985-998.

Bayat M, Daneshjoo F, Nisticò N, (2017), "The effect of different intensity measures and earthquake directions on the seismic assessment of skewed highway bridges," *Earthquake Engineering and Engineering Vibration*, **16**(1): 165–179.

Bar-Sever YE, Kroger PM, Borjesson JA (1998), "Estimating Horizontal Gradients of Tropospheric Path Delay with a single GPS Receiver", *Journal Geophysical Research*, **103**: 5019-5035.

Bertiger W, Desai SD, Haines B, Harvey N, Moore AW, Owen S, Weiss JP (2010), "Single receiver phase ambiguity resolution with GPS data," *Journal of Geodesy*, **84**: 327-337.

Bournas DA, Negro P, Taucer FF (2014), "Performance of industrial buildings during the Emilia earthquakes in Northern Italy and recommendations for their strengthening," *Bulletin Earthquake Engineering*, **12**: 2383–2404.

Breuer P, Chmielewski T, Górski P, Konopka E, Tarczyński L (2015), "Monitoring horizontal displacements in a vertical profile of a tall industrial chimney using Global Positioning System technology for detecting dynamic characteristics," *Structural Control and Health Monitoring*, **22**(7): 1002–1023.

Bhagat S, Wijeyewickrema AC (2017), "Seismic response evaluation of base-isolated reinforced concrete buildings under bidirectional excitation," *Earthquake Engineering and Engineering Vibration*, **16**(2): 365-382.

CEN (2004), *European Prestandard ENV 1998-1-4: Eurocode 8 – Design of structures for earthquake resistance, Part 1-4: Strengthening and repair of buildings*, Comite European de Normalisation, Brussels.

Chalaha F, Chalah-Rezguia L, Faleka K, Djellaba SE, Abderrahim Balib A (2014), "Fundamental vibration period of SW buildings," *APCBEE Procedia*, **9:** 354-359.

Chopra AK (1995), *Dynamics of structures: theory and applications to earthquake engineering*, Prentice-Hall, Inc., Upper Saddle River, N.J.

D.M. 19 Giugno 1984 (1984), *Norme tecniche relative alle costruzioni sismiche (Technicals regulations for to seismic constructions)*, Gazzetta Ufficiale (Ufficial document of the Italian Government) n° 208-30/07/1984.

Goel RK, Chopra AK (1997), "Period formulas for moment-resisting frame buildings," *Structural Engineering Division ASCE*, **123**: 1454-1461.

Gurtner W (1995), "Guidelines for a Permanent EUREF GPS Network," *Proceedings of EUREF Symposium*, Helsinki, Finland, May 1995, EUREF Publication No. 4, Editor E. Gubler and H. Hornik, on-line at http://www.epncb.oma.be/papers.html.

Hao C, Quancai X, Boyang D, Haoyu Z, Hongfu C. (2016), "Seismic Damage to Structures in the Ms6.5 Ludian Earthquake," *Earthquake Engineering and Engineering Vibration*, **15**(1): 173–186.

Hong L, Hwang W (2000), "Empirical formula for fundamental vibration periods of reinforced concrete buildings in Taiwan," *Earthquake Engineering and Structural Dynamics*, **29**: 327-333.

Kedar S, Hajj GA, Wilson BD, Heflin MB (2003), "The effect of the second order GPS ionospheric correction on receiver positions", *Geophysical Research Letters*, **30**(16): 1829.

Kobori T, Yamaguchi Y, Nakashima S, Shimizu N (2015), "Continuous displacement monitoring of rockfill dam during earthquakes by using global positioning system," *Journal of Japan Society of Dam Engineers*, **25**(1): 6-15.

Li XJ, Rizos C, Ge LL, Ambikairajah E., Tamura Y., Yoshida A. (2006), "Building monitors: the complementary characteristics of GPS and accelerometers in monitoring structural deformation," *Inside GNSS*, **21**: 40-47.

Moschas F, Stiros SC (2011), "Measurement of the dynamic displacements and of the modal frequencies of a short-span pedestrian bridge using GPS and an accelerometer", *Engineering Structures*, **33**(1): 10-17.

Moschas F, Stiros SC (2013), "Three-dimensional dynamic deflections and natural frequencies of a stiff footbridge based on measurements of collocated sensors," *Structural Control and Health Monitoring*, **21**(1): 23–42.

Moschas F, Avallone A, Saltogianni V, Stiros SC (2014), "Strong motion displacement waveforms using 10-Hz precise point positioning GPS: an assessment based on free oscillation experiments," *Earthquake Engineering & Structural Dynamics*, **43**(12): 1853–1866.

Moschas F, Stiros SC (2015a), "Dynamic deflections of a stiff footbridge using 100-Hz GNSS and accelerometer data," *Journal of Surveying Engineering*, **141**(4): ID 04015003.

Moschas F, Stiros SC (2015b), "PLL bandwidth and noise in 100 Hz GPS measurements," *Journal GPS Solutions*, **19**(2): 173-185.

NEHRP (1994), *Recommended provisions for the development of seismic regulations for new buildings*, Building Seismic Safety Council, Washington, D.C., 1994.

NTC (2008), *Norme tecniche per le costruzioni (Technicals regulations for buildings)* Gazzetta Ufficiale (Ufficial document of the Italian Government) n° 153- 02/07/2008.

Pondrelli S, Salimbeni S, Perfetti P, Danecek P (2012), "Quick regional centroid moment tensor solutions for the Emilia 2012 (northern Italy) seismic sequence," *Annals of Geophysics*, **55**(4): 615-621.

Psimoulis P, Pytharouli S, Karambalis D, Stiros SC (2008), "Potential of Global Positioning System (GPS) to measure frequencies of oscillations of engineering structures," *Journal of Sound and Vibration*, **318**(3): 606–623.

Psimoulis P, Houlie N, Meindl M, Rothacher M (2015), "Consistency of PPP GPS and strong-motion records: case study of Mw 9.0 Tohoku-Oki 2011 earthquake," *Smart Structures and Systems*, **16**(2): 347-366.

Schaal RE, Larocca APC (2009), "Measuring dynamic oscillations of a small span cable-stayed footbridge: Case study using L1 GPS receivers," *Journal of Surveying Engineering*, **135**(1): 33-37.

Scognamiglio L, Margheriti L, Mele FM, Tinti E, Bono A, De Gori P, Lauciani V, Lucente FP, Mandiello AG, Marcocci C, Mazza S, Pintore S, Quintiliani M (2012), "The 2012 Pianura Padana Emiliana seismic sequence: locations, moment tensors and magnitudes," *Annals of Geophysics*, **55**(4): 549-559.

SEAOC (1996), *Recommended lateral force requirements and commentary*, Seismological Engineers Association of California, San Francisco, California.

Yi TH, Li HN, Gu M *et al.* (2009), "Ambient vibration study for real time monitoring of suspension bridge using GPS," *Proceedings of the 4th International Conference on Structural Health Monitoring on Intelligent Infrastructure* (*SHMII-4*), Zurich, Switzerland, 2009.

Yi TH, Li HN, Gu M (2010a) "Recent research and applications of GPS based technology for bridge health monitoring," *Science China Technological Sciences*, **53**(10): 2597–2610.

Yi TH, Li HN, Gu M (2010b), "Full scale measurement of dynamic response of a suspension bridge subjected to environmental loads using GPS technology," *Science China Technological Sciences*, **53**(2): 469–479.

Yi TH, Li HN, Gu M (2011), "Characterization and extraction of global positioning system multipath signals using an improved particle-filtering algorithm," *Measurements Science and Technology*, **22**(7): 1-11.

Yi TH, Li HN, Gu M (2012), "Effect of different construction materials on propagation of GPS monitoring signals," *Measurement*, **45**(5): 1126-1139.

Yi TH, Li HN, Gu M (2013a) "Recent research and applications of GPS based monitoring technology for high-rise structures," *Structural Control and Health Monitoring*, **20**(5): 649–670.

Yi TH, Li HN, Gu M (2013b), "Experimental assessment of high-rate GPS receivers for deformation monitoring of bridge," *Measurement*, **46**(1): 420-432.

Yi TH, Li HN, Gu M (2013c), "Wavelet based multi-step filtering method for bridge health monitoring using GPS and accelerometer," *Smart Structures and Systems*, **11**(4): 331-348.

Wang G (2011), "GPS landslide monitoring: single base vs. network solutions—a case study based on the Puerto Rico and Virgin Islands permanent GPS network," *Journal of Geodetic Science*, **1**(3): 191-203.

Webb FH, Zumberge JF (1996), *An introduction to GIPSY/OASIS-II: precision software for the analysis of data from the Global Positioning System*, Ed. JPL D-11088, July 1996.

Yigit CO, Gurlek E (2017), "Experimental testing of high-rate GNSS precise point positioning (PPP) method for detecting dynamic vertical displacement response of engineering structures," *Geomatics, Natural Hazards and Risk*, **1**: 1-12.

Yigit CO (2016), "Experimental assessment of post-processed kinematic Precise Point Positioning method for structural health monitoring," *Geomatics, Natural Hazards and Risk*, **7**(1): 360-383.

Zumberge J, Heflin M, Jefferson D, Watkins M, Webb F (1997), "Precise point positioning for the efficient and robust analysis of GPS data from large networks," *Journal Geophysical Research*, **102**: 5005-5017.